ISSN: 0067-2904

The Dynamics of Modified Leslie-Gower Predator-Prey Model Under the Influence of Nonlinear Harvesting and Fear Effect

Saad Al-Momen*, Raid Kamil Naji
Department of Mathematics, College of Science, University of Baghdad, Iraq

Received: 1/12/2021 Accepted: 31/12/2021

Abstract

A modified Leslie-Gower predator-prey model with fear effect and nonlinear harvesting is developed and investigated in this study. The predator is supposed to feed on the prey using Holling type-II functional response. The goal is to see how fear of predation and presence of harvesting affect the model's dynamics. The system's positivity and boundlessness are demonstrated. All conceivable equilibria's existence and stability requirements are established. All sorts of local bifurcation occurrence conditions are presented. Extensive numerical simulations of the proposed model are shown in form of Phase portraits and direction fields. That is to guarantee the correctness of the theoretical results of the dynamic behavior of the system and to confirm the existence of various forms of bifurcations. The fear rate is observed to have a stabilizing effect up to a threshold value, after which it leads to prey extinction. The harvesting coefficients, on the other hand, serve as control parameters that, when exceeded, trigger the system to extinction.

Keywords: predator-prey, Modified Leslie-Gower, local stability, fear effect, nonlinear harvesting, bifurcation analysis.

ديناميكية نموذج ليزلي– جاورالمعدل للمفترس – الفريسة تحت تأثير الحصاد غير الخطي وتأثير الخوف

سعد محمد علي المؤمن*، رائد كامل ناجي
قسم الرياضيات، كلية العلوم، جامعة بغداد، بغداد، العراق

الخلاصة

طور ونوقش نموذج ليزلي – جاور المعدل للمفترس والفريسة مع تأثير الخوف والحصاد غير الخطي في هذه الدراسة. افترضنا أن يتغذى المفترس على الفريسة استنادا الى الاستجابة الوظيفية من النوع الثاني لهولينج. الهدف هو معرفة تأثير الخوف من الافتراس ووجود الحصاد على ديناميكيات النموذج. اثبتت إيجابية النظام وعدم حدوده ووضع جميع متطلبات وجود واستقرار نقاط التوازن الممكنة. كما قدمت جميع شروط حدوث أنواع التشعب المحلي. لضمان التحقق من صحة النتائج النظرية للسلوك الديناميكي للنظام وتأكيد وجود أشكال مختلفة من التشعبات اجرينا محاكاة عددية واسعة النطاق للنموذج المقترح ومثلت بشكل صور الطور وحقول الاتجاه. لوحظ أن معدل الخوف له تأثير استقرار يصل إلى قيمة عتبة ، وبعد ذلك يؤدي إلى انقراض الفريسة. من ناحية أخرى ، تعمل معاملات الحصاد كمعايير تحكم تؤدي، عند تجاوزها حدا معين، إلى انقراض النظام.

*Email: saad.m@sc.uobaghdad.edu.iq

1. Introduction

One of the most popular subjects in biomathematics is population dynamics. The study of the evolution of diverse populations has always been of special interest, beginning with populations of a single species and progressing to more realistic models in which several species exist and interact in the same ecosystem. Models that explore competitive interactions, symbiosis, commensalism, or predator-prey dynamics are some of them. The predator-prey model has been extensively studied by mathematical and biological researchers since its introduction made by Alfred J. Lotka in 1925 and Vito Volterra [1] in 1926. They described the interaction between two species combined with the predator-prey relationship, where they define the problem with a system of polynomial differential equations of degree two. The importance of this problem lies in understanding the dynamics between two species (a predator and prey) that live together in the same environment and looking for suitable conditions that allow both species to survive in equilibria.

Later, applications of these systems began to increase. New applications on population dynamics had been developed, and these systems have also been utilized to represent a variety of other natural phenomena.

Besides the basic relationship given by the Lotka-Volterra model; many factors may affect species growth. So, this model was developed by many researchers taking into consideration various environmental factors that affect the existence and stability of this system, such as prey refuge [2-4], disease [5, 6], delay [7], harvesting [7-9], Allee effect [4, 10, 11], age structure [12], sex structure and sexual favoritism [13], seasonal variation [14], and many other factors.

The functional response is an essential part of the predator-prey model, which describes the change in prey number killed per individual predator per unit of time as a consequence of changes in prey density. The most commonly used functional response in the existing literature is a function of prey's density only (Holling I-III) [2, 4, 15, 16], in which interfering among predators is not utilized whereas this will be common when predators contest for food. To address this important factor, functional responses (ratio-dependent [17], Beddington-DeAngelis [18], and Crowley-Martin [7] have been developed which do not rely just on the density of the prey but rather on the density of both prey and predator.

While many predator-prey models considered a logistic growth of predators, Leslie and Gower [19] assumed that the predator grows logistically, where its carrying capacity is proportional to the density of prey $hy\left(1-\frac{y}{\alpha x}\right)$ where x and y are the populations of prey and predator respectively. The term $\frac{y}{\alpha x}$ is called Leslie-Gower term.

On the other hand, predators can devour other populations when food is scarce, but their growth will be limited since their primary prey is scarce. To consider this issue, Aziz-Alaoui and Okiye [20] suggested a modified Leslie–Gower model by introducing a constant b in the denominator of Leslie-Gower term that measures environmental protection for the predator $\frac{y}{b+\alpha x}$ to avoid singularities when $x=0$. Since then, many researchers have examined the modified Leslie–Gower models with a variety of functional responses [2, 21-23], harvesting [7, 22] Allee effect [24], etc.

Moreover, from a financial income point of view, it is significant to consider the harvesting of species in predator-prey models. In the literature, several types of harvesting strategies have been utilized. Some of them used constant harvesting, $h(x)=h$ [25], proportional harvesting $h(x)=Ex$ [26] where x is the population that presents the harvesting (prey or predator), age-selective harvesting [27], while others considered nonlinear harvesting [7]. Nonlinear harvesting is more relevant than other approaches from both a financial and biological point of view [23, 28]. Many researchers consider Holling type II harvesting $h(x)=\frac{qEx}{m_1E+m_2x}$. For

example, Gupta et al worked with a model with Holling type II harvesting in prey [23] and Holling type II harvesting in predator in [29].

Another factor to consider is that in some environments, prey may be afraid of predators and respond appropriately, making predator hunting more difficult. Due to fear of predation risk, the prey population can change its feeding area to a safer place and sacrifice their highest intake rate areas, increase their vigilance, regulate their strategies for reproduction, etc. In recent years, many experts began to study the predator-prey model with fear effect; see [3, 6]

The dynamics and bifurcations of a modified Leslie-Gower predator-prey model with Holling-II functional response and nonlinear harvesting in both the prey and predator communities are investigated in this paper, as well as the influence of the fear factor.

2. Mathematical Model Formulation

The study considers a predator-prey problem, with $N(T)$ and $P(T)$, respectively, representing prey and predator population densities at time T. Resource-consumer, plant-herbivore, parasite-host, tumor cells (virus)-immune system, susceptible-infectious interactions, and so on are examples.

In the proposed model, prey population $N(T)$ is considered logistically growing in absence of predator $P(T)$ with a birth rate r_1 and level of fear induced by predator population K such that:

$$\frac{dN}{dT} = \frac{r_1 N}{1+KP} - dN - a_1 N^2. \quad (1)$$

The morality density is represented by the term dN, where d is the natural death rate of prey. Also, the term $a_1 N^2$ is added to consider competition between prey community members, where a_1 is the intraspecific competition.

Moreover, the interaction between prey and predator is assumed to follow Holling-II functional response. According to these considerations, the change in the density of prey takes the following form in the presence of the predator:

$$\frac{dN}{dT} = \frac{r_1 N}{1+KP} - dN - a_1 N^2 - \frac{bmNP}{c_1+mN}, \quad (2)$$

where b represents the maximum attack rate, c_1 represents the half-saturation constant of predation and the parameter $m \in (0,1)$ represents the availability constant rate of prey for predation due to the assumption of the existence of a $(1-m)$ constant rate of prey's refuge in the environment.

The density of predator population is assumed to follow the modified Leslie–Gower predation as follows:

$$\frac{dP}{dT} = r_2 P\left[1 - \frac{a_2 P}{c_2+mN}\right] \quad (3)$$

where the parameter r_2 represents the intrinsic growth rates of the predator, a_2 is the maximum value which per capita reduction rate of P can attend, and c_2 is the carrying capacity of the predator in the absence of the prey.

In the proposed model, prey and predator are assumed to follow nonlinear harvesting with the harvesting function of Holling-II. The harvesting of prey is presented by the term $\frac{q_1 EmN}{p_1 E+p_2 mN}$, while that of predator is represented by the term $\frac{q_2 EP}{p_3 E+p_4 P}$, where $q_i, (i=1,2)$ are the catchability coefficient of prey and predator respectively, E is the effort made to harvest individuals and $p_i, (i=1,2,3,4)$: suitable constants. It's worth noting that the effort represented by E in both equations is considered to be the same for both species, making this model more appropriate for aquatic environments.

Combining all the above assumptions give the following set of dynamical differential equations:

$$\begin{aligned}\frac{dN}{dT} &= \frac{r_1 N}{1+KP} - dN - a_1 N^2 - \frac{bmNP}{c_1+mN} - \frac{q_1 EmN}{p_1 E + p_2 mN},\\ \frac{dP}{dT} &= r_2 P\left[1 - \frac{a_2 P}{c_2+mN}\right] - \frac{q_2 EP}{p_3 E + p_4 P},\end{aligned} \tag{4}$$

where all of the parameters are assumed to be positive and described as above.

Note that, using the scaling variables $r_1 T = t$, $x = \frac{a_1}{r_1} N$, and $y = \frac{b a_1}{r_1^2} P$ in the system (4) reduces the number of parameters from 17 to 12 parameters and the system (4) takes the following dimensionless form:

$$\begin{aligned}\frac{dx}{dt} &= x\left[\frac{1}{1+k_1 y} - k_2 - x - \frac{my}{k_3+mx} - \frac{k_4 Em}{k_5 E + mx}\right] := x f_1(x,y),\\ \frac{dy}{dt} &= y\left[k_6\left(1 - \frac{k_7 y}{k_8+mx}\right) - \frac{k_9 E}{k_{10}E + y}\right] := y f_2(x,y),\end{aligned} \tag{5}$$

with the initial conditions:

$$x(0) = x_0 \geq 0,\ y(0) = y_0 \geq 0, \tag{6}$$

and the dimensionless parameters are given by:

$$\begin{aligned}&k_1 = \frac{K r_1^2}{b a_1},\ k_2 = \frac{d}{r_1},\ k_3 = \frac{a_1 c_1}{r_1},\ k_4 = \frac{a_1 q_1}{r_1^2 p_2},\ k_5 = \frac{p_1 a_1}{p_2 r_1},\\ &k_6 = \frac{r_2}{r_1},\ k_7 = \frac{a_2 r_1}{b},\ k_8 = \frac{a_1 c_2}{r_1},\ k_9 = \frac{b a_1 q_2}{p_{4 r_1^3}},\ k_{10} = \frac{b a_1 p_3}{p_4 r_1^2}.\end{aligned}$$

Note that, since the right-hand side of the interaction functions of the system (5) are continuous and have continuous partial derivatives, then system (5) has a unique solution that belongs to the positive quadrant $\mathbb{R}_+^2$.

3. Positivity and Boundedness

Theorem (1) and theorem (2) below prove that the model formulation is ecologically relevant by showing that solutions of system (5) together with the initial condition (6) are positive and uniformly bounded.

Theorem 1: *All solutions of system (5) with initial conditions (6) remain positive forever.*

Proof: The proof is direct and hence it is omitted.

Theorem 2: *All the solutions of system (5) with initial conditions (6) are uniformly bounded.*

Proof: From the system (5),

$$\begin{aligned}\frac{dx}{dt} &\leq \frac{x}{1+k_1 y} - k_2 x - x^2\\ &\leq x - k_2 x - x^2\\ &= x[(1-k_2) - x],\end{aligned}$$

and this shows that the solution of the system $x(t) \leq 1 - k_2 := M_1$ as $t \to \infty$, by lemma 2 in (23). Clearly, due to the survival condition of the prey in the absence of a predator, we have always that $1 - k_2 > 0$.

Now substituting the maximum value M_1 in the second equation of system (5) gives that:

$$\frac{dy}{dt} \leq k_6 y\left(1 - \frac{k_7 y}{k_8 + m M_1}\right).$$

Then, by solving the above differential inequality, it is observed that:

$$y(t) \leq \frac{k_8 + m M_1}{k_7} := M_2 \text{ as } t \to \infty.$$

which proves the boundedness of all the solutions. □

4. Existence and the Stability of Equilibria

The presence of equilibrium points of the dimensionless system, as well as a qualitative analysis of their stability, are investigated in this section.

The number of equilibrium points of system (5) depends on the parameter values. For example, Figure 1 shows that for the set of parameter values given in Table 1, the system has one trivial, one predator-free, one prey-free, and one interior equilibrium point. While, for set

of parameter values given in Table 2, the system has one trivial, one predator-free, two prey free and two interior equilibrium points.

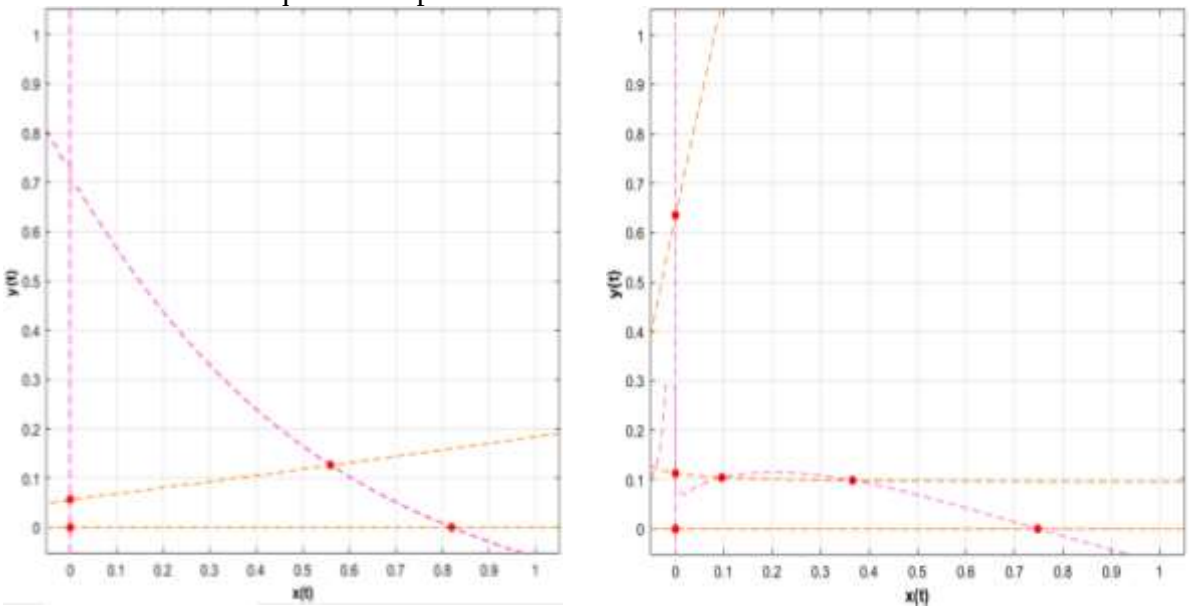

(a) **(b)**

Figure 1- The number of equilibrium points of the system (5) **(a)** there are 4 equilibrium points for set #1 of parameter values given in Table 1 **(b)** there are 6 equilibrium points for set #2 of parameter values given in Table 2.

4.1 Trivial Equilibrium Point

It is clear that the trivial equilibrium point $E_0(0,0)$ at the origin is always exists.

4.2 Predator Free Equilibrium Points

The boundary equilibria on $x-$axis are calculated by solving the following quadratic equation:

$$E\big(k_4m + k_5(k_2-1)\big) + \big(Ek_5 + m(k_2-1)\big)x + mx^2 = 0. \quad (7)$$

The roots of Eq. (7) depend on the parameters k_2, k_4, k_5, m and E, so according to Descartes's rule there are the following cases:

Case 1. There is no equilibrium point with $k_2 \geq 1$, since the prey survives if the natural mortality rate is lower than the birth rate.

Case 2. When $k_2 < 1$

a. If both $k_4m > k_5(1-k_2)$ and $Ek_5 + m(k_2-1) > 0$, then there is no equilibrium point.

b. If $k_4m > k_5(1-k_2)$ and $Ek_5 + m(k_2-1) < 0$, then either there is no equilibrium point or there are two equilibrium points $E_1(x_1, 0)$ and $E_2(x_2, 0)$ where x_1 and x_2 are the positive roots of Eq. (7) with $x_1 < x_2$ and are given by

$$x_1 = \frac{-\big(Ek_5+m(k_2-1)\big)-\sqrt{\big(Ek_5+m(k_2-1)\big)^2-4Em\big(k_4m+k_5(k_2-1)\big)}}{2m}.$$

$$x_2 = \frac{-\big(Ek_5+m(k_2-1)\big)+\sqrt{\big(Ek_5+m(k_2-1)\big)^2-4Em\big(k_4m+k_5(k_2-1)\big)}}{2m}.$$

c. If $k_4m + k_5(k_2-1) < 0$, then only $E_2(x_2, 0)$ exits.

4.3 Prey Free Equilibrium Points

The boundary equilibria on $y-$axis are calculated by solving the following quadratic equation:

$$Ek_8(k_9 - k_6k_{10}) + k_6(Ek_7k_{10} - k_8)y + k_6k_7y^2 = 0. \quad (8)$$

The roots of Eq. (8) depend on the parameters $k_6, k_7, k_8, k_9, k_{10}$ and E, so according to Descartes's rule there are the following cases:

Case 1. If both $k_9 > k_6k_{10}$ and $Ek_7k_{10} > k_8$ there is no equilibrium point.

Case 2. If both $k_9 > k_6k_{10}$ and $Ek_7k_{10} < k_8$, then either there is no equilibrium point or there are two equilibrium points $E_3(0, y_3)$ and $E_4(0, y_4)$ where y_3 and y_4 are the positive roots of Eq. (8) with $y_3 < y_4$ and are given by

$$y_3 = \frac{k_6(k_8 - Ek_7k_{10}) - \sqrt{{k_6}^2(Ek_7k_{10} - k_8)^2 - 4Ek_6k_7k_8(k_9 - k_6k_{10})}}{2k_6k_7}.$$

$$y_4 = \frac{k_6(k_8 - Ek_7k_{10}) + \sqrt{{k_6}^2(Ek_7k_{10} - k_8)^2 - 4Ek_6k_7k_8(k_9 - k_6k_{10})}}{2k_6k_7}.$$

Case 3. If $k_9 < k_6k_{10}$, then only $E_4(0, y_4)$ exits.

4.4 Interior Equilibrium Points

The positive interior points are found by solving system (5) for $x > 0$ and $y > 0$. It is obtained that:

$$x^* = \frac{(A_1 - A_2) + (B_1 - B_2)y^* + Cy^{*2}}{(D_1 - D_2) + Fy^*}, \tag{9}$$

where $A_1 = Ek_8k_9$, $A_2 = Ek_6k_8k_{10}$, $B_1 = Ek_6k_7k_{10}$, $B_2 = k_6k_8$, $C = k_6k_7$, $D_1 = Emk_6k_{10}$, $D_2 = Emk_9$ and $F = mk_6$. It is clear that each one of them has a positive value. However, y^* is the positive root of the polynomial (10) below:

$$\alpha_0 + \alpha_1 y^* + \alpha_2 y^{*2} + \alpha_3 y^{*3} + \alpha_4 y^{*4} + \alpha_5 y^{*5} + \alpha_6 y^{*6} + \alpha_7 y^{*7} = 0, \tag{10}$$

where the polynomial coefficients $\alpha_i; i = 0,1, \dots, 7$ are depending on the system parameters with $\alpha_7 = -C^3m^2k_1$ is negative, while all other coefficients of Eq. (10) could be positive or negative. Therefore, if $\alpha_0 > 0$ then there exists at least one positive equilibrium point $E^*(x^*, y^*)$.

5. Stability Analysis of Equilibria

In this section, the nonlinear system (5) is linearized around each equilibrium point using the Jacobian matrix to investigate the local stability of various equilibrium points.

The Jacobian matrix of system (5) about an arbitrary point (x, y) is determined by:

$$J(x, y) = \begin{bmatrix} x\frac{\partial f_1}{\partial x} + f_1 & x\frac{\partial f_1}{\partial y} \\ y\frac{\partial f_2}{\partial x} & y\frac{\partial f_2}{\partial y} + f_2 \end{bmatrix}, \tag{11}$$

where

$$\frac{\partial f_1}{\partial x} = \frac{Ek_4m^2}{(Ek_5 + mx)^2} + \frac{m^2y}{(k_3 + mx)^2} - 1,$$
$$\frac{\partial f_1}{\partial y} = -\left(\frac{m}{k_3 + mx} + \frac{k_1}{(1 + k_1y)^2}\right),$$
$$\frac{\partial f_2}{\partial x} = \frac{k_6k_7my}{(k_8 + mx)^2},$$
$$\frac{\partial f_2}{\partial y} = \frac{Ek_9}{(Ek_{10} + y)^2} - \frac{k_6k_7}{k_8 + mx}.$$

Recall that, if all eigenvalues of the Jacobian matrix at an equilibrium point have negative real parts then this point is locally asymptotically stable. Accordingly, the following theorems present the local stability conditions for each of the above equilibria.

Theorem 3: *The trivial equilibrium point E_0 is:*

i. Local asymptotically stable node if $k_5(1 - k_2) < k_4m$ and $k_6k_{10} < k_9$.

ii. Saddle point if either $k_5(1 - k_2) < k_4m$ and $k_6k_{10} > k_9$ or $k_5(1 - k_2) > k_4m$ and $k_6k_{10} < k_9$.

iii. Unstable node if $k_5(1 - k_2) > k_4m$ and $k_6k_{10} > k_9$.

Proof: Depending on the general Jacobian matrix that given by (11), the Jacobian matrix at $E_0(0,0)$ is given by:

$$J(0,0) = \begin{bmatrix} 1 - k_2 - \frac{k_4 m}{k_5} & 0 \\ 0 & k_6 - \frac{k_9}{k_{10}} \end{bmatrix}.$$

The eigenvalues of $J(0,0)$ are $\lambda_1 = \frac{k_5(1-k_2)-k_4 m}{k_5}$, and $\lambda_2 = \frac{k_6 k_{10}-k_9}{k_{10}}$. So, if (i) holds the two eigenvalues are negative, and then E_0 is local asymptotically stable. If the condition in (ii) holds, then λ_1 and λ_2 have opposite signs, hence E_0 is saddle-node. Finally, if the condition in (iii) holds, then both eigenvalues are positive, hence the point E_0 is unstable node. □

Theorem 4: *If any of the predator-free equilibrium points $E_i(x_i, 0)$, $(i = 1,2)$ exists, then it is:*

i. Local asymptotically stable node if $Ek_4m^2 < (Ek_5 + mx_i)^2$ and $k_6k_{10} < k_9$.
ii. Saddle point if either $Ek_4m^2 < (Ek_5 + mx_i)^2$ and $k_6k_{10} > k_9$ or $Ek_4m^2 > (Ek_5 + mx_i)^2$ and $k_6k_{10} < k_9$.
iii. Unstable node if $Ek_4m^2 > (Ek_5 + mx_i)^2$ and $k_6k_{10} > k_9$.

Proof: At $E_i(x_i, 0), (i = 1,2)$, the Jacobian matrix can be written as

$$J(x_i, 0) = \begin{bmatrix} x_i\left(\frac{Ek_4m^2}{(Ek_5+mx_i)^2} - 1\right) & -x_i\left(k_1 + \frac{m}{k_3+mx_i}\right) \\ 0 & k_6 - \frac{k_9}{k_{10}} \end{bmatrix},$$

Therefore, the eigenvalues of $J(x_i, 0), (i = 1,2)$ are given by:

$$\lambda_1 = \frac{\left(Ek_4m^2-(Ek_5+mx_i)^2\right)x_i}{(Ek_5+mx_i)^2} \text{ and } \lambda_2 = \frac{k_6k_{10}-k_9}{k_{10}}$$

Hence, if the condition (i) holds, the two eigenvalues are negative and $E_i, (i = 1,2)$ is local asymptotically stable. If the condition (ii) holds, then λ_1 and λ_2 have opposite signs, hence $E_i, (i = 1,2)$ is saddle-node. Finally, if condition (iii) holds, then both eigenvalues are positive, hence the point is an unstable node. □

Theorem 5: *If any of the prey free equilibrium points $E_i(0, y_i)$, $(i = 3,4)$ exists, then it is:*

i. Local asymptotically stable node if $k_3k_5 < R_1$ and $Ek_8k_9 < R_2$.
ii. Saddle point if either $k_3k_5 < R_1$ and $Ek_8k_9 > R_2$ or $k_3k_5 > R_1$ and $Ek_8k_9 < R_2$.
iii. Unstable node if $k_3k_5 > R_1$ and $Ek_8k_9 > R_2$.

where $R_1 = \left(k_2k_3k_5 + m(k_3k_4 + k_5y_i)\right)(1 + k_1y_i)$, $R_2 = k_6k_7(Ek_1 + y_i)^2$.

Proof: At $E_i(0, y_i)$, $(i = 3,4)$, the Jacobian matrix is given by

$$J(0, y_i) = \begin{bmatrix} \frac{1}{1 + k_1y_i} - k_2 - \frac{k_4 m}{k_5} - \frac{my_i}{k_3} & 0 \\ \frac{k_6k_7my_i^2}{k_8^2} & y_i\left(\frac{Ek_9}{(Ek_{10} + y_i)^2} - \frac{k_6k_7}{k_8}\right) \end{bmatrix}$$

Clearly, the eigenvalues of $J(0, y_i)$, $(i = 3,4)$ are:

$$\lambda_1 = \frac{k_3k_5-\left(k_2k_3k_5+m(k_3k_4+k_5y_i)\right)(1+k_1y_i)}{k_3k_5(1+k_1y_i)} \text{ and } \lambda_2 = \frac{\left(Ek_8k_9-k_6k_7(Ek_{10}+y_i)^2\right)y_i}{k_8(Ek_{10}+y_i)^2}$$

Hence, if the condition (i) holds, the two eigenvalues are negative and $E_i(0, y_i)$, $(i = 3,4)$ is local asymptotically stable. If the condition (ii) holds, then λ_1 and λ_2 have opposite signs, hence $E_i(0, y_i)$, $(i = 3,4)$ is saddle-node. Finally, if condition (iii) holds, then both eigenvalues are positive, hence the point is an unstable node. □

Theorem 6: *If any interior equilibrium point $E^*(x^*, y^*)$ exists, then this point is:*

i. Saddle point if $\frac{Ek_4m^2}{(Ek_5+mx^*)^2} + \frac{m^2y^*}{(k_3+mx^*)^2} - 1$ and $\frac{Ek_9}{(Ek_{10}+y^*)^2} - \frac{k_6k_7}{k_8+mx^*}$ have opposite signs, and $j_{11}j_{22} < j_{12}j_{21}$.

ii. Unstable node if $\frac{Ek_4m^2}{(Ek_5+mx^*)^2}+\frac{m^2y^*}{(k_3+mx^*)^2}-1$ *and* $\frac{Ek_9}{(Ek_{10}+y^*)^2}-\frac{k_6k_7}{k_8+mx^*}$ *have the same signs and* $T(J^*)>0$.

iii. Stable node if $\frac{Ek_4m^2}{(Ek_5+mx^*)^2}+\frac{m^2y^*}{(k_3+mx^*)^2}-1$ *and* $\frac{Ek_9}{(Ek_{10}+y^*)^2}-\frac{k_6k_7}{k_8+mx^*}$ *have the same signs and* $T(J^*)<0$.

where $T(J^*)$ *is trace of the Jacobian matrix at this point* $E^*(x^*,y^*)$.

Proof: At $E^*(x^*,y^*)$, the Jacobian matrix is given by:

$$J(x^*,y^*)=\begin{bmatrix} x^*\left(\frac{Ek_4m^2}{(Ek_5+mx^*)^2}+\frac{m^2y^*}{(k_3+mx^*)^2}-1\right) & -x^*\left(\frac{k_1}{(1+k_1y^*)^2}+\frac{m}{k_3+mx^*}\right) \\ \frac{k_6k_7my^{*2}}{(k_8+mx^*)^2} & y^*\left(\frac{Ek_9}{(Ek_{10}+y^*)^2}-\frac{k_6k_7}{k_8+mx^*}\right)\end{bmatrix}=[j_{ij}].$$

If the condition (i) holds, then $j_{11}j_{22}<0$ and it is clear that $j_{12}j_{21}<0 \Rightarrow |J(x^*,y^*)|<0$ $\Rightarrow E^*$ is a saddle point. If the condition (ii) holds, then $j_{11}j_{22}>0 \Rightarrow |J(x^*,y^*)|>0 \Rightarrow E^*$is unstable node when $T(J^*)>0$. Similarly, E^* is stable node when $T(J^*)<0$. □

6. Bifurcation Analysis

This section is dedicated to study some potential bifurcation scenarios at the stable equilibrium points of the system (5) when the parameter values are varied.

System (5) can be rewritten in the following vector forms to simplify the notations:

$$\frac{dX}{dt}=F(X), \text{ with } X=\begin{bmatrix}x\\y\end{bmatrix}, \text{ and } F=\begin{bmatrix}xf_1(x,y)\\yf_2(x,y)\end{bmatrix}.$$

Then the second derivate of F with respect to X can be expressed as:

$$D^2F(X)(V,V)=\begin{bmatrix}\frac{2k_1^2v_2^2x}{(1+k_1y)^3}-\frac{2k_3mv_1v_2}{(k_3+mx)^2}-\frac{2k_1v_1v_2}{(1+k_1y)^2}+2v_1^2\left(m^2\left(\frac{E^2k_4k_5}{(Ek_5+mx)^3}+\frac{k_3y}{(k_3+mx)^3}\right)-1\right)\\ \frac{2E^2k_{10}k_9v_2^2}{(Ek_{10}+y)^3}-\frac{2k_6k_7(k_8v_2+mv_2x-mv_1y)^2}{(k_8+mx)^3}\end{bmatrix}, \quad (12a)$$

where $V=(v_1,v_2)^T$ is a general vector. Furthermore, we have

$$D^3F(X)(V,V,V)=\begin{bmatrix}6\left(\frac{k_3^2m^2v_1^2v_2}{(k_3+mx)^4}-\frac{E^2k_4k_5m^3v_1^3}{(Ek_5+mx)^4}+\frac{k_3m^3v_1^2(v_2x-v_1y)}{(k_3+mx)^4}+\frac{k_1^2v_2^2(v_1-k_1v_2x+k_1v_1y)}{(1+k_1y)^4}\right)\\ \frac{6k_6k_7mv_1(k_8v_2+mv_2x-mv_1y)^2}{(k_8+mx)^4}-\frac{6E^2k_{10}k_9v_2^3}{(Ek_{10}+y)^4}\end{bmatrix}. \quad (12b)$$

Theorem 7: *If the parameter* k_6 *passes through the value* $k_6^*=\frac{k_9}{k_{10}}$ *and* $k_5(1-k_2)<k_4m$, *then system (5) at the trivial equilibrium point* E_0 *has*

i. No saddle-node bifurcation.

ii. Transcritical bifurcation provided that

$$k_8 \neq Ek_7k_{10}. \quad (13)$$

iii. A pitchfork bifurcation otherwise.

Proof: At E_0, the Jacobian matrix of system (5) with $k_6=k_6^*$ becomes:

$$J_0=DF(E_0,k_6^*)=\begin{bmatrix}1-k_2-\frac{k_4m}{k_5} & 0\\ 0 & 0\end{bmatrix}.$$

Clearly, J_0 has a zero eigenvalue with another negative eigenvalue, and the corresponding eigenvector for the zero eigenvalue can be written as:

$$U_1=\begin{bmatrix}0\\1\end{bmatrix}.$$

While the eigenvector corresponding to the zero eigenvalue of ${J_0}^T$ is determined as:

$$W_1=\begin{bmatrix}0\\1\end{bmatrix}.$$

Differentiating F with respect to k_6 gives:

$$F_{k_6} = \begin{bmatrix} 0 \\ y\left(1 - \frac{k_7 y}{k_8 + mx}\right) \end{bmatrix}.$$

Therefore, straightforward computation shows that:

$$W_1^T F_{k_6}(E_0, k_6^*) = 0.$$

Consequently, by Sotomayor's theorem, system (5) has no saddle-node bifurcation near E_0 and $k_6 = k_6^*$. Moreover, direct computation gives that:

$$W_1^T \left[DF_{k_6}(E_0, k_6^*)U_1\right] = 1 \neq 0.$$

Also, using the form of D^2F given by equation (12a), and the eigenvectors U_1 with W_1 gives that:

$$W_1^T [D^2F(E_0, k_6^*)(U_1, U_1)] = \frac{2k_9(k_8 - Ek_7k_{10})}{Ek_8k_{10}^2}.$$

Therefore, condition (13) guarantees that $W_1^T [D^2F(E_0, k_6^*)(U_1, U_1)] \neq 0$. Hence, by Sotomayor's theorem, a transcritical bifurcation takes place.

Otherwise, $W_1^T [D^2F(E_0, k_6^*)(U_1, U_1)] = 0$. In addition, using the form of D^3F given by equation (12b), and the eigenvectors U_1 with W_1 gives that:

$$W_1^T [D^3F(E_0, k_6^*)(U_1, U_1, U_1)] = -\frac{6k_9}{E^2k_{10}^3} \neq 0.$$

Hence, a pitchfork bifurcation takes place, and the proof is complete. □

Theorem 8: *Assume that* $Ek_4m^2 < (Ek_5 + mx_i)^2$ near any of the predator-free equilibrium points $E_i(x_i, 0)$, $(i = 1,2)$, then if the parameter k_6 passes through the value $k_6^* = \frac{k_9}{k_{10}}$, then the system (5) at this equilibrium point has

i. No saddle-node bifurcation.

ii. Transcritical bifurcation provided that

$$\frac{1}{E} \neq \frac{k_{10}k_7}{k_8 + mx_i}. \quad (14)$$

iii. A pitchfork bifurcation otherwise.

Proof: At $E_i(x_i, 0)$, $(i = 1,2)$, the Jacobian matrix of system (5) with $k_6 = k_6^*$ becomes:

$$J_i = DF(E_i, k_6^*) = \begin{bmatrix} x_i\left(\frac{Ek_4m^2}{(Ek_5 + mx_i)^2} - 1\right) & -x_i\left(k_1 + \frac{m}{k_3 + mx_i}\right) \\ 0 & 0 \end{bmatrix}.$$

Clearly, J_i has a zero eigenvalue with another negative eigenvalue, and the corresponding eigenvector for the zero eigenvalue can be written as:

$$U_2 = \begin{bmatrix} C_1 \\ 1 \end{bmatrix}.$$

where

$$C_1 = \frac{(Ek_5 + mx_i)^2[m + k_1(k_3 + mx_i)]}{(k_3 + mx_i)[Ek_4m^2 - (Ek_5 + mx_i)^2]}.$$

Clearly $C_1 < 0$, due to given condition.

While the eigenvector corresponding to the zero eigenvalue of ${J_i}^T$ is determined as:

$$W_2 = \begin{bmatrix} 0 \\ 1 \end{bmatrix}.$$

And,

$$W_2^T F_{k_6}(E_i, k_6^*) = 0.$$

Consequently, by Sotomayor's theorem, system (5) has no saddle-node bifurcation near E_i and $k_6 = k_6^*$. Moreover, direct computation gives that:

$$W_2^T \left[DF_{k_6}(E_i, k_6^*)U_2\right] = 1 \neq 0.$$

Also, using the form of D^2F given by equation (12a), and the eigenvectors U_2 with W_2 gives that:

$$W_2^T [D^2F(E_i, k_6^*)(U_2, U_2)] = \frac{2k_9}{k_{10}^2}\left(\frac{1}{E} - \frac{k_{10}k_7}{k_8 + mx_i}\right).$$

Therefore, condition (14) guarantees that $W_2^T[D^2F(E_i,k_6^*)(U_2,U_2)] \neq 0$. Hence, by Sotomayor's theorem, a transcritical bifurcation takes place.

Moreover, if condition (14) does not satisfy, then we have $W_2^T[D^2F(E_i,k_6^*)(U_2,U_2)] = 0$. In addition, using the form of D^3F given by equation (12b), and the eigenvectors U_2 with W_2 gives that:

$$W_2^T[D^3F(E_i,k_6^*)(U_2,U_2,U_2)] = \frac{6k_9}{k_{10}}\left[\frac{k_6k_7mC_1}{k_9(k_8+mx_i)^2} - \frac{1}{E^2{k_{10}}^2}\right] \neq 0.$$

Hence, a pitchfork bifurcation takes place, and the proof is complete. □

Theorem 9: Assume that $Ek_8k_9 < k_6k_7(Ek_1+y_i)^2$ *near any of the prey free equilibrium points* $E_i(0,y_i)$, $(i=1,2)$, *then if the parameter* k_2 *passes through the value* $k_2^* = \frac{1}{1+k_1y_i} - \frac{k_4m}{k_5} - \frac{my_i}{k_3}$, *then system (5) at this equilibrium point has*

i. No saddle-node bifurcation.

ii. Transcritical bifurcation provided that

$$B_2 \neq 0 \tag{15}$$

where

$$B_2 = Ek_3k_5^2(m(1+k_1y_i)^2 + k_1k_3) - C_2(1+k_1y_i)^2\left(m^2\left({k_3}^2k_5 + Ek_5{}^2y_i\right) - Ek_3{}^2{k_5}^2\right).$$

iii. A pitchfork bifurcation if condition (15) does not satisfy and

$$\frac{m^2{C_2}^2}{{k_3}^2} - \frac{k_4m^3{C_2}^3}{E^2{k_5}^3} - \frac{m^3{C_2}^3y_i}{{k_3}^3} + \frac{k_1^2C_2}{(1+k_1y_i)^3} \neq 0. \tag{16}$$

Proof: At $E_i(0,y_i)$, $(i=3,4)$, the Jacobian matrix of system (5) with $k_2 = k_2^*$ becomes:

$$J_i = DF(E_i,k_2^*) = \begin{bmatrix} 0 & 0 \\ \frac{k_6k_7my_i^2}{k_8^2} & y_i\left(\frac{Ek_9}{(Ek_{10}+y_i)^2} - \frac{k_6k_7}{k_8}\right) \end{bmatrix}.$$

Clearly J_i has a zero eigenvalue with another negative eigenvalue, and the corresponding eigenvector for the zero eigenvalue can be written as:

$$U_3 = \begin{bmatrix} C_2 \\ 1 \end{bmatrix}.$$

where

$$C_2 = k_8\frac{k_6k_7(Ek_{10}+y_i)^2 - Ek_8k_9}{k_6k_7my_i(Ek_{10}+y_i)^2}.$$

Clearly $C_2 > 0$, due to given condition.

While the eigenvector corresponding to the zero eigenvalue of ${J_i}^T$ is determined as:

$$W_3 = \begin{bmatrix} 1 \\ 0 \end{bmatrix}.$$

And,

$$W_3^T F_{k_2}(E_i,k_2^*) = 0.$$

Consequently, by Sotomayor's theorem, system (5) has no saddle-node bifurcation near E_i and $k_2 = k_2^*$. Moreover, direct computation gives that:

$$W_3^T\left[DF_{k_2}(E_i,k_2^*)U_3\right] = -C_2 \neq 0.$$

Also, using the form of D^2F given by equation (12a), and the eigenvectors U_3 with W_3 gives that:

$$W_3^T[D^2F(E_i,k_2^*)(U_3,U_3)] = \frac{-2C_2B_2}{Ek_3{}^3k_5{}^2(1+k_1y_i)^2}.$$

Therefore, condition (15) guarantees that $W_3^T[D^2F(E_i,k_2^*)(U_3,U_3)] \neq 0$. Hence, by Sotomayor's theorem, a transcritical bifurcation takes place.

Moreover, if condition (15) does not satisfy, then we have $W_3^T[D^2F(E_i,k_2^*)(U_3,U_3)] = 0$. In addition, using the form of D^3F given by equation (12b), and the eigenvectors U_3 with W_3 gives that:

$$W_3^T[D^3F(E_i,k_2^*)(U_3,U_3,U_3)] = 6\left(\frac{m^2{C_2}^2}{{k_3}^2} - \frac{k_4m^3{C_2}^3}{E^2{k_5}^3} - \frac{m^3{C_2}^3y_i}{{k_3}^3} + \frac{k_1^2C_2}{(1+k_1y_i)^3}\right).$$

Note that, condition (16) guarantees that $W_3^T[D^3F(E_i,k_2^*)(U_3,U_3,U_3)] \neq 0$. Hence, a pitchfork bifurcation takes place, and the proof is complete. □

Theorem 10: *Assume that* $\frac{Ek_4m^2}{(Ek_5+mx^*)^2}+\frac{m^2y^*}{(k_3+mx^*)^2}<1$ *and* $\frac{Ek_9}{(Ek_{10}+y^*)^2}>\frac{k_6k_7}{k_8+mx^*}$ *near the any of the interior equilibrium points* $E^*(x^*,y^*)$*, then if the parameter* k_6 *passes through the value:*

$k_6{}^{**}=\frac{j_{11}Ek_9(k_8+mx^*)^2}{k_7\,(Ek_{10}+y^*)^2(my^*j_{12}+(k_8+mx^*)j_{11})}$,

Then system (5) at this equilibrium point has saddle-node bifurcation provided that:

$$\frac{mk_7y^{*2}}{(k_8+mx^*)^2}C_3+1-\frac{2k_7y^*}{k_8+mx^*}\neq 0, \tag{17}$$

$$C_4\delta_{11}+\delta_{21}\neq 0, \tag{18}$$

where all new symbols are given in the proof.

Proof: Consider the Jacobian matrix of system (5) at E^* with $k_6=k_6{}^{**}$ that can be written as:

$$J_*(E^*,k_6{}^{**})=\begin{bmatrix} j_{11} & j_{12} \\ j_{21}{}^* & j_{22}{}^* \end{bmatrix}.$$

where

$$j_{11}=x^*\left(\frac{Ek_4m^2}{(Ek_5+mx^*)^2}+\frac{m^2y^*}{(k_3+mx^*)^2}-1\right),\ j_{12}=-x^*\left(\frac{k_1}{(1+k_1y^*)^2}+\frac{m}{k_3+mx^*}\right),$$

$$j_{21}{}^*=\frac{k_6{}^{**}k_7my^{*2}}{(k_8+mx^*)^2},\ \ j_{22}{}^*=y^*\left(\frac{Ek_9}{(Ek_{10}+y^*)^2}-\frac{k_6{}^{**}k_7}{k_8+mx^*}\right).$$

Straightforward computation shows that $|J_*|=j_{11}j_{22}{}^*-j_{12}j_{21}{}^*=0$, and hence J_* has a zero eigenvalue, and the corresponding eigenvector for this eigenvalue can be written as:

$$U_4=\begin{bmatrix} C_3 \\ 1 \end{bmatrix}.$$

where

$$C_3=-\frac{j_{12}}{j_{11}}<0.$$

While the eigenvector corresponding to the zero eigenvalue of $J_*{}^T$ is determined as:

$$W_4=\begin{bmatrix} C_4 \\ 1 \end{bmatrix}.$$

where

$$C_4=-\frac{j_{21}{}^*}{j_{11}}>0.$$

And,

$$W_4^TF_{k_6}(E^*,k_6{}^{**})=y^*\left(1-\frac{k_7y^*}{k_8+mx^*}\right)\neq 0.$$

Consequently, by Sotomayor's theorem, system (5) satisfies the first condition of saddle-node bifurcation near E^* and $k_6{}^{**}$. Moreover, direct computation with the use of conditions (17) and (18) gives that:

$$W_4^T\left[DF_{k_6}(E^*,k_6{}^{**})U_4\right]=\frac{mk_7y^{*2}}{(k_8+mx^*)^2}C_3+1-\frac{2k_7y^*}{k_8+mx^*}\neq 0.$$

$$W_4^T[D^2F(E^*,k_6{}^{**})(U_4,U_4)]=C_4\delta_{11}+\delta_{21}\neq 0$$

where

$$\delta_{11}=\frac{2k_1^2x^*}{(1+k_1y^*)^3}-\frac{2k_3mC_3}{(k_3+mx^*)^2}-\frac{2k_1C_3}{(1+k_1y^*)^2}+2C_3{}^2\left[m^2\left(\frac{E^2k_4k_5}{(Ek_5+mx^*)^3}+\frac{k_3y^*}{(k_3+mx^*)^3}\right)-1\right],$$

$$\delta_{21}=\frac{2E^2k_{10}k_9}{(Ek_{10}+y^*)^3}-\frac{2k_6{}^{**}k_7(k_8+mx^*-mC_3y^*)^2}{(k_8+mx^*)^3},$$

represent the elements of $D^2F(E^*,k_6{}^{**})(U_4,U_4)$. Hence, a saddle node bifurcation takes place, and the proof is complete. □

7. Numerical Analysis

The overall dynamics of system (5) are numerically investigated in this section for various sets of initial values and parameter values. This study aims to demonstrate the impacts of changing parameter values on the system's dynamical behavior and to validate the theoretical results achieved. The numerical simulations are carried out using a combination of parameter values given in Table (1) and Table (2).

Table 1- Set #1 of parameter values

Parameter:	k_1	k_2	k_3	k_4	k_5	k_6	k_7	k_8	k_9	k_{10}	E	m
Value:	2.35	0.13	0.47	0.3	0.61	0.87	0.79	0.06	0.1	0.4	0.92	0.12

Table 2- Set #2 of parameter values

Parameter:	k_1	k_2	k_3	k_4	k_5	k_6	k_7	k_8	k_9	k_{10}	E	m
Value:	2.37	0.24	0.13	0.08	0.1	0.1	0.17	0.13	0.1	0.15	0.11	0.75

As previously mentioned in section 4, there is a various number of equilibrium points for different values of parameters. Figure 1 shows two examples of that.

Now, using the parameters given in Table 1 with various sets of initial points, system (5) is solved numerically, and then the trajectories that have been obtained are drawn in form of direction field and phase portrait as shown in Figure 2. It is clear from this figure that there are 4 equilibrium points: one trivial, one predator-free, one prey-free, and one interior equilibrium point. The interior equilibrium point is stable (spiral sink), while the others are unstable.

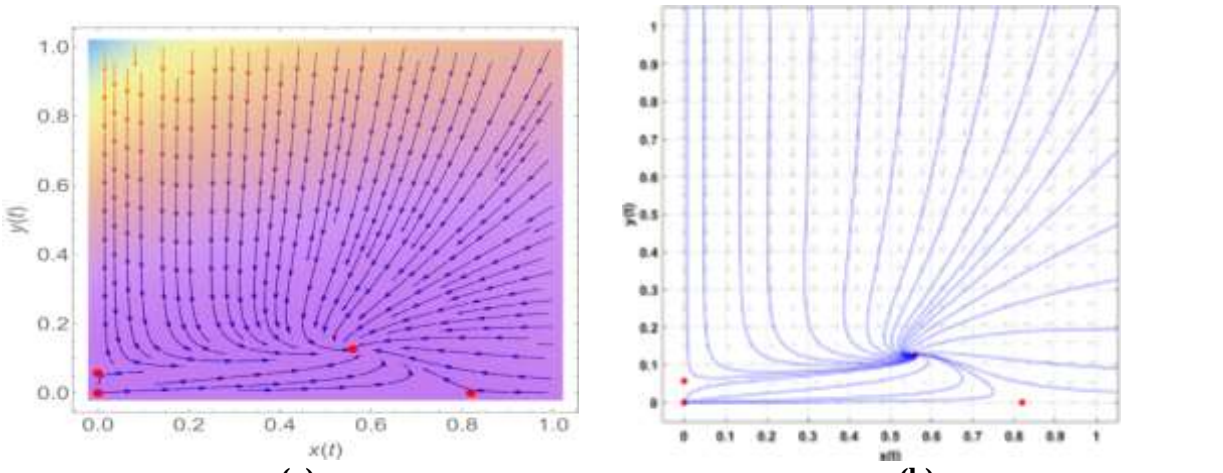

(a) **(b)**

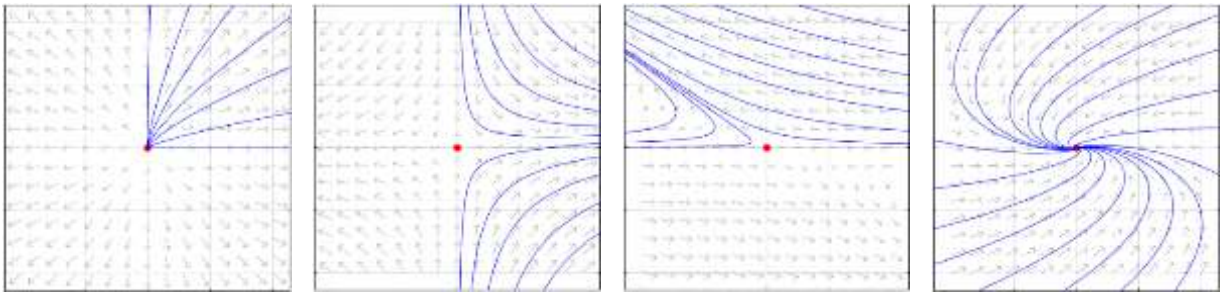

(c) **Trivial equilibrium point (0,0) nodal**

(d) **Prey free equilibrium point (0,0.057543)**

(e) **Predator free equilibrium point**

(f) **Interior equilibrium point**

source	**saddle point**	**(0.81979,0) saddle point**	**(0.559785,0.126559) spiral sink**

Figure 2- For the parameters given in Table (1) with different initial points **(a)** The direction field of the system (5) **(b)** The phase portrait of the trajectories of the system (5) **(c)-(f)** The dynamic behavior near the 4 equilibrium points.

Three different initial points near the interior equilibrium point are selected randomly and then the time series for the obtained trajectories of system (5) are drawn in Figures 3. The trajectories of system (5) approach to that point as shown in Figure 3.

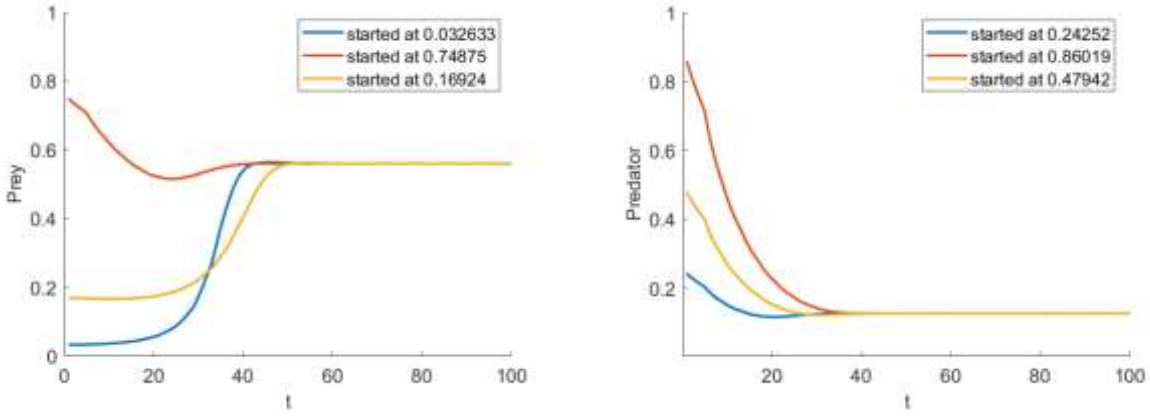

(a) **(b)**

Figure 3- The solutions of system (5) approaches asymptotically to the interior point (0.559785,0.126559) using parameters in Table (1) (a) Prey trajectories (b) Predator trajectories as a function of time.

Figure 4 shows that by putting $k_6^* = \frac{k_9}{k_{10}}$ and keeping the values of other parameters in Table (1), then instead of four equilibrium points, system (5) will have just two: the trivial and the predator-free equilibrium points. Both of them are nonhyperbolic equilibrium points. This agrees with the results of both Theorem 7 and Theorem 8.

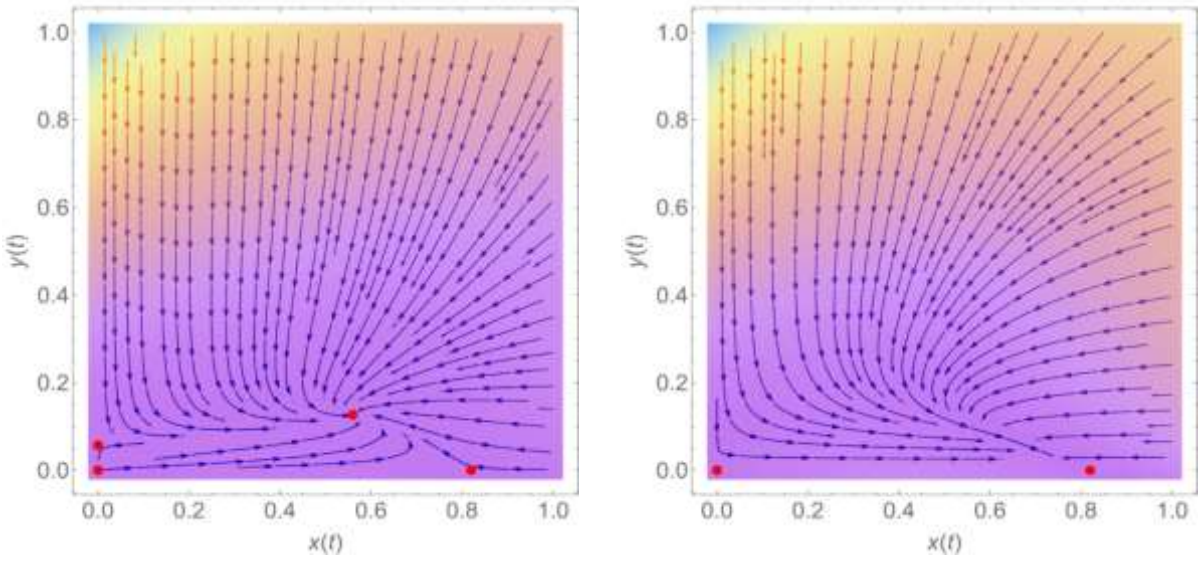

(a) **(b)**

Figure 4-The dynamical behavior of system (5) with parameter values in Table (1) **(a)** when $k_6^* > \frac{k_9}{k_{10}} = 0.25$ **(b)** when $k_6^* \leq \frac{k_9}{k_{10}} = 0.25$.

Figure (5) shows that by putting $k_2^* \geq \frac{1}{1+k_1 y_i} - \frac{k_4 m}{k_5} - \frac{m y_i}{k_3} = 0.81$ and keeping the value of other parameters in Table 1 then instead of four equilibrium points, system (5) will have three equilibrium points: the trivial, one predator-free, and one prey-free equilibrium point. Moreover, the prey-free equilibrium point will change its behavior from saddle-node to nodal sink. This agrees with the result of Theorem 9.

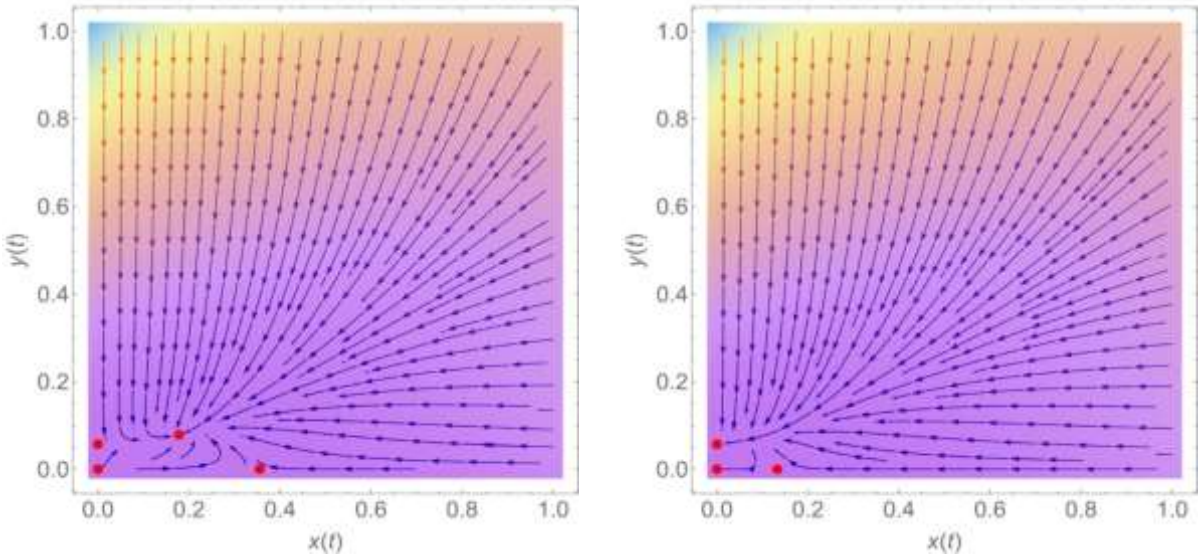

(a) **(b)**

Figure 5- The dynamical behavior of system (5) with parameter values in Table-1 **(a)** when $k_2^* < \frac{1}{1+k_1 y_i} - \frac{k_4 m}{k_5} - \frac{m y_i}{k_3} = 0.81$ **(b)** when $k_2^* \geq \frac{1}{1+k_1 y_i} - \frac{k_4 m}{k_5} - \frac{m y_i}{k_3} = 0.81$.

As mentioned previously, system (5) has a rich dynamic behavior, for example, Figure (6) shows the behavior of the system under influence of set #2 of parameter values which are given in Table 2. In this case, there are six equilibrium points: (i) one trivial saddle equilibrium point (ii) one predator-free nodal sink (iii) two prey-free equilibrium points, one of them is saddle point and the other is a nodal sink (iv) two interior equilibrium points, one spiral source and the other is a saddle point.

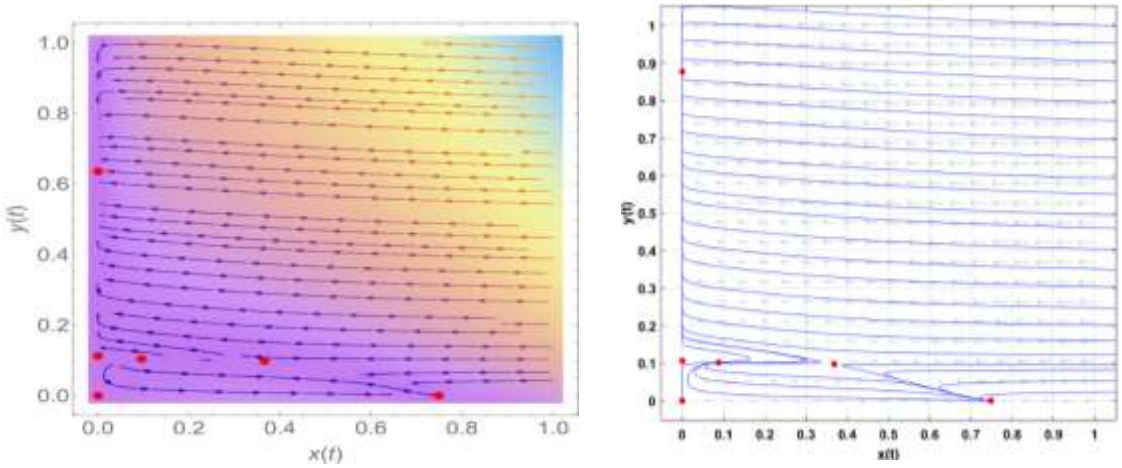

(a) **(b)**

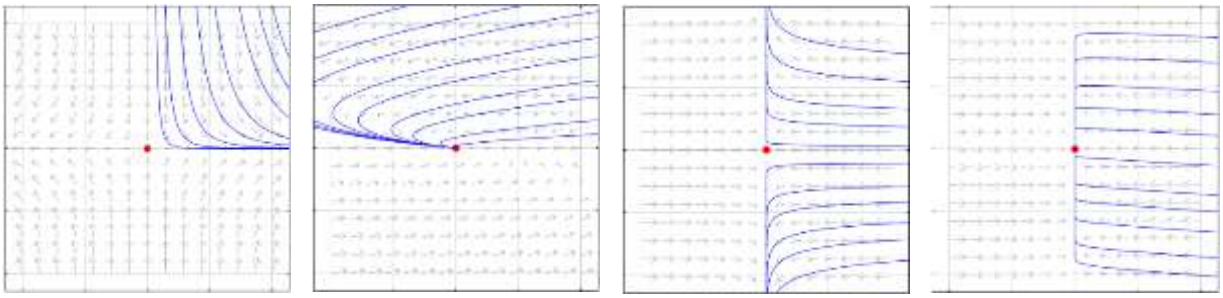

(c)
Trivial equilibrium point (0,0) saddle point

(d)
Predator free equilibrium point (0.74847,0) nodal sink

(e)
Prey free equilibrium point (0,010663) saddle point

(f)
Prey free equilibrium point (0,0.87687) nodal sink

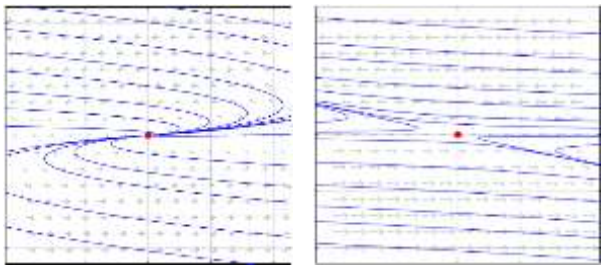

(g)
Interior equilibrium point (0.88011,0.10225) spiral source

(h)
Interior equilibrium point (0.36854,0.097753) saddle point

Figure 6-For the parameters given in Table 2 with different initial points **(a)** The direction field of the system (5) **(b)** The phase portrait of the trajectories of system (5) **(c)-(f)** The dynamic behavior near the 4 boundary equilibrium points. **(g)-(h)** The dynamic behavior near the 2 interior equilibrium points.

Figure 7 shows that for set #1, as the value of the level of fear induced by predator population (k_1) increases, the unique interior equilibrium point converges to the prey-free equilibrium point and preserves its behavior as a spiral sink. While Figure 8 shows that for set #2 with an increase in the level of fear induced by predator population (k_1), the two interior equilibrium points converge to each other and then unify and disappear. When these two points exist, they

preserve their behavior, the right one is always saddle-node while the left one is always a spiral source.

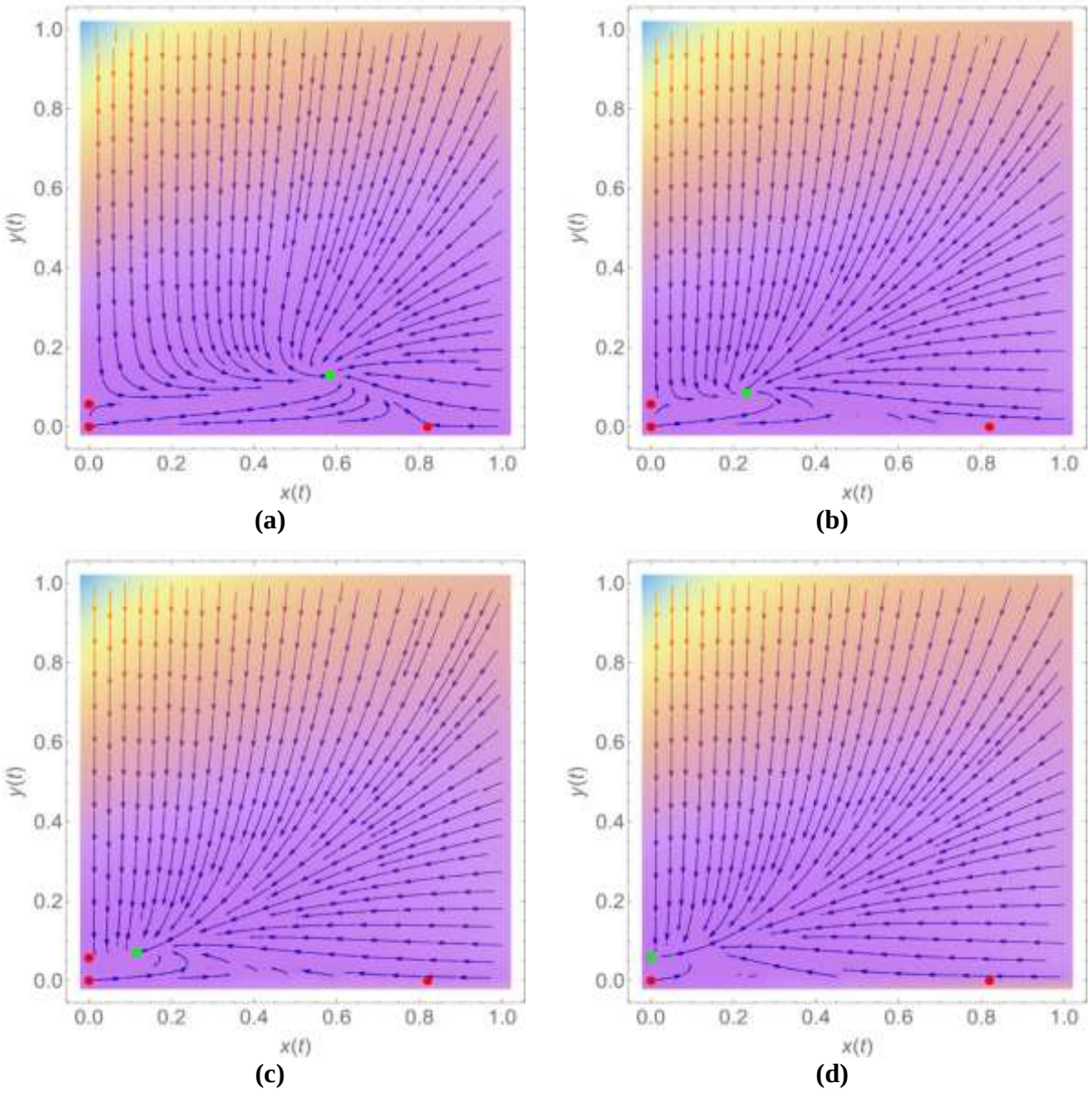

Figure 7- The interior equilibrium point of set #1 (the point in green) converges to the prey-free equilibrium point with the increase of the value of k_1 **(a)** $k_1 = 2$ **(b)** $k_1 = 15$ **(c)** $k_1 = 30$ **(d)** $k_1 = 68$.

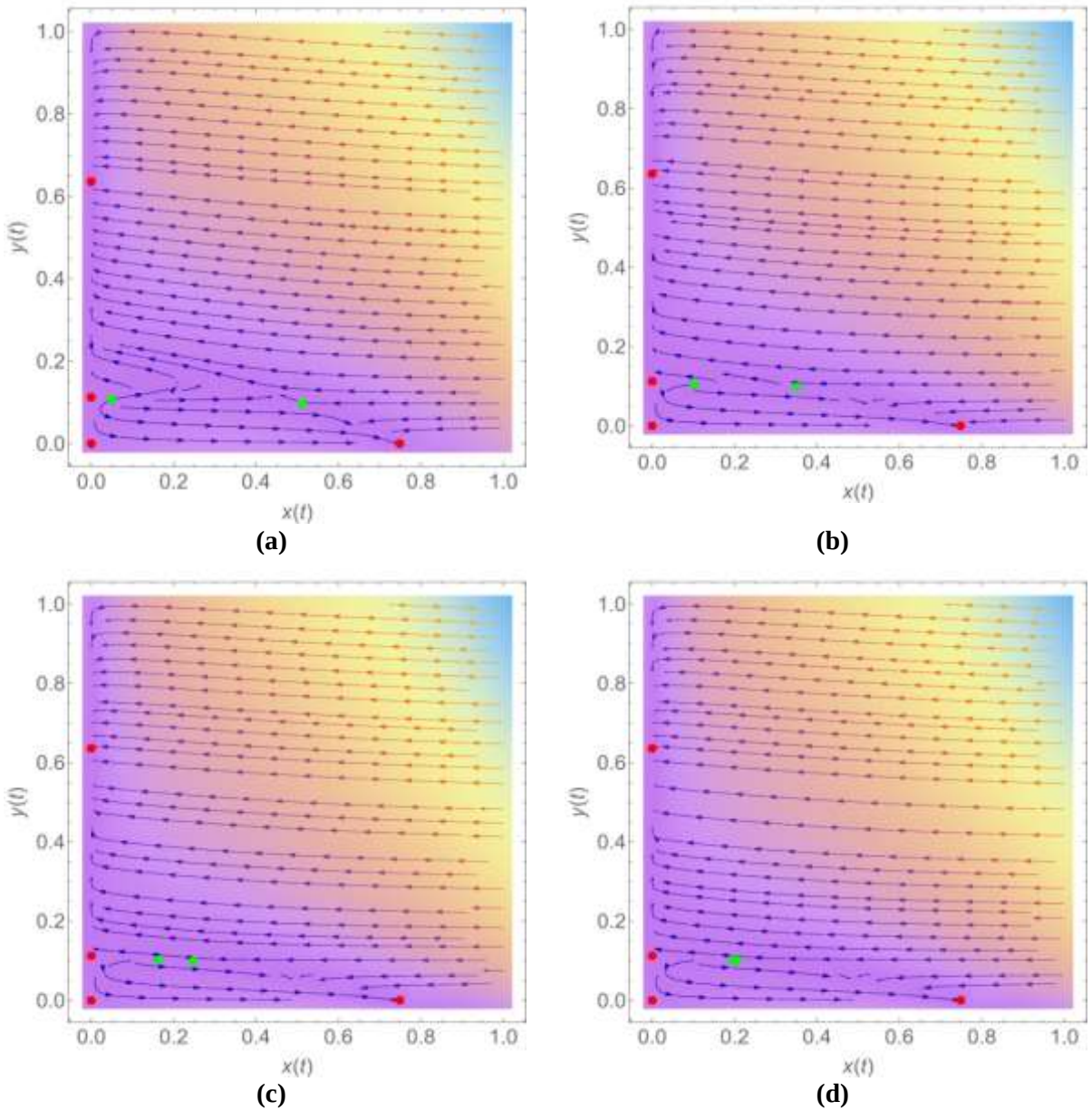

Figure 8-The two interior equilibrium points of set #2 (the points in green) converge to each other with the increase of the value of k_1 **(a)** $k_1 = 1$ **(b)** $k_1 = 2.5$ **(c)** $k_1 = 3.2$ **(d)** $k_1 = 3.3$.

Moreover, to explore the effect of harvesting, Figure 9 shows that for set #1, as the value of the catchability coefficient of prey (k_4) increases, the unique interior equilibrium point converges to the prey-free equilibrium point and preserves its behavior as a spiral sink. While Figure 10 shows that for set #2, the two interior equilibrium points converge to each other and then unify and disappear. When these two points exist, they preserve their behavior, the right one is always saddle-node while the left one is always a spiral source.

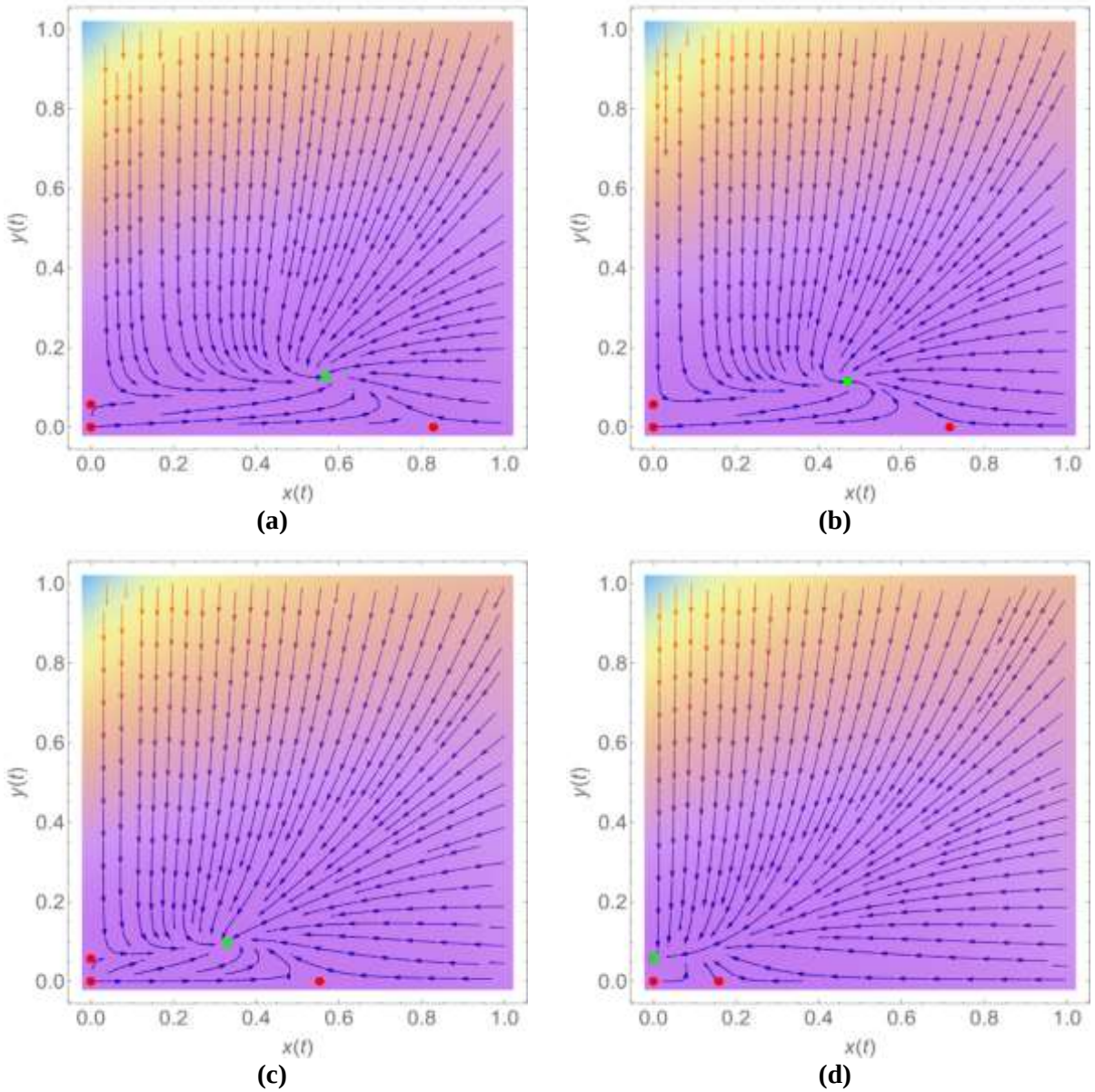

Figure 9-The interior equilibrium point of set #1 (the point in green) converges to the prey-free equilibrium point with the increase of the value of k_4 **(a)** $k_4 = 0.25$ **(b)** $k_4 = 0.9$ **(c)** $k_4 = 1.8$ **(d)** $k_4 = 3.74$.

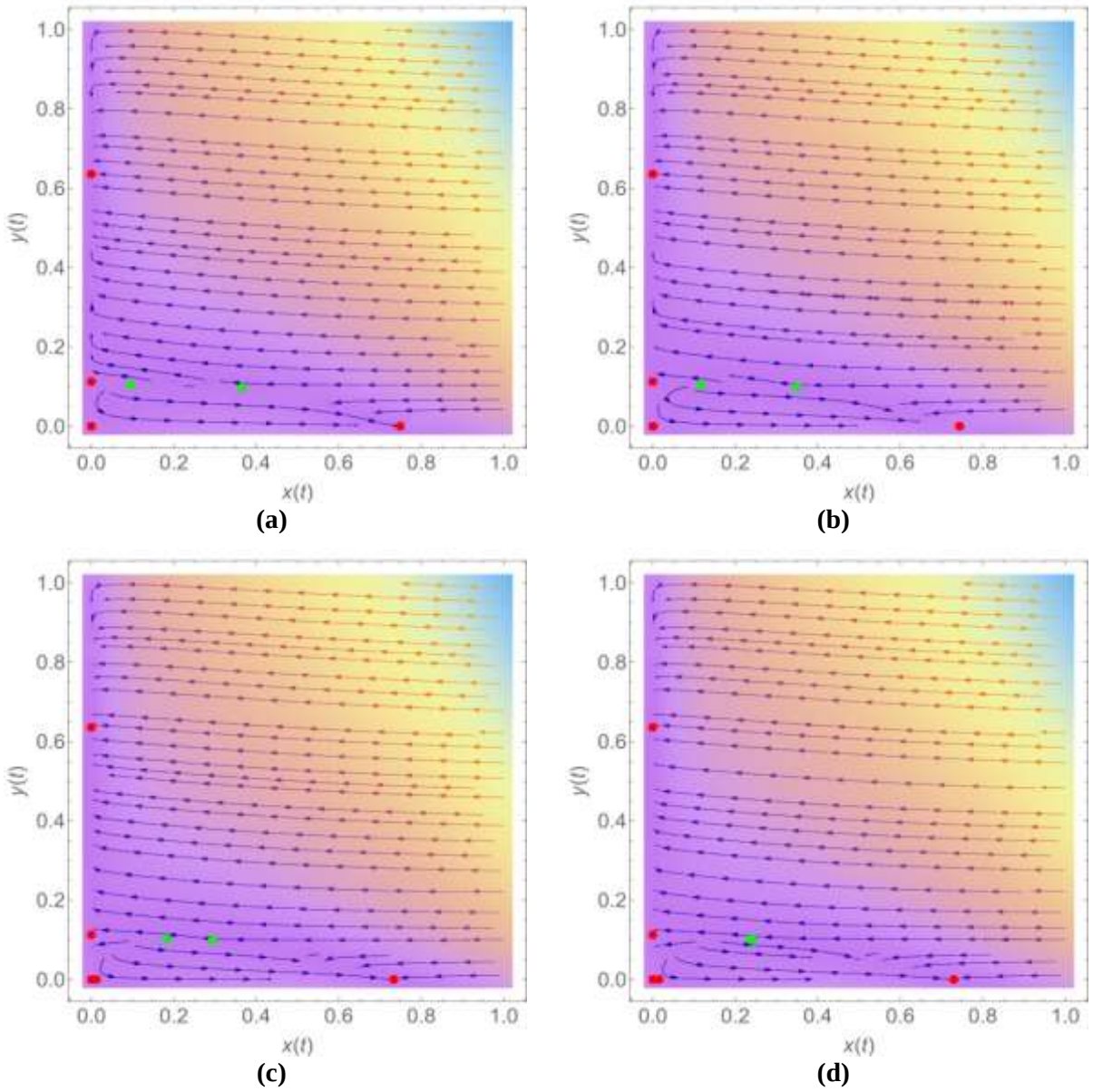

Figure 10-The two interior equilibrium points of set #2 (the points in green) converge to each other with the increasing of the value of k_4 **(a)** $k_4 = 0.08$ **(b)** $k_4 = 0.11$ **(c)** $k_4 = 0.18$ **(d)** $k_4 = 0.2013$.

Also, Figure 11 shows that for set #1, as the value of the catchability coefficient of predator (k_9) increases, the unique interior equilibrium point converges to predator-free equilibrium point and preserves its behavior as a spiral sink. At the same time, for set #2, the two interior equilibrium points follow a similar scenario to that appear in Figures 8 and 10, where the two points combine with each other and then disappear. On the other hand, decreasing the value of this parameter toward zero makes the right interior equilibrium point goes toward the predator-free equilibrium point, while the left interior equilibrium point goes toward the prey-free equilibrium point and then toward the trivial equilibrium point as shown in Figure 12.

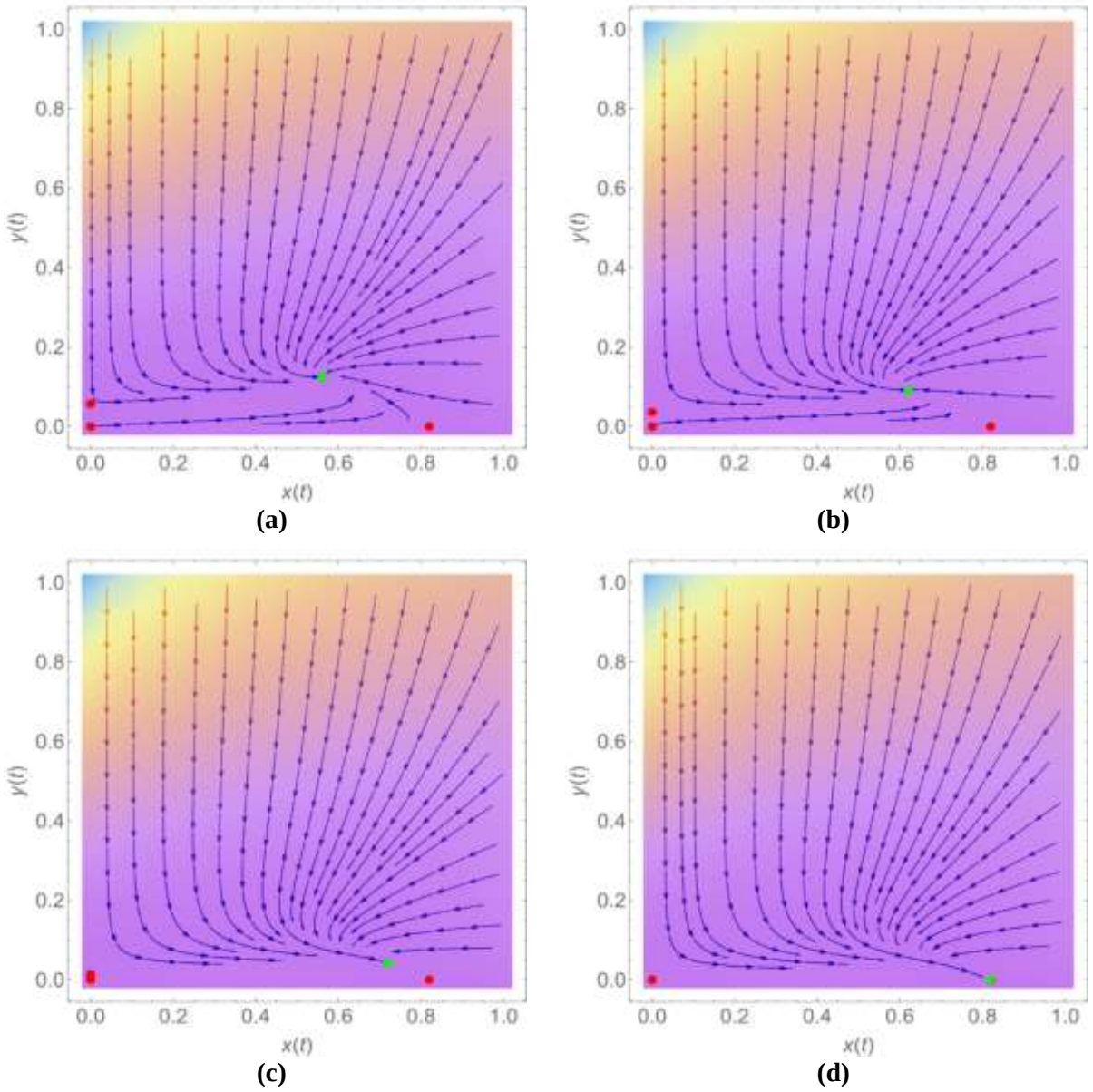

Figure 11- The interior equilibrium point of set #1 (the point in green) approaches the predator-free equilibrium point with the increase of the value of k_9 **(a)** $k_9 = 0.1$ **(b)** $k_9 = 0.2$ **(c)** $k_9 = 0.3$ **(d)** $k_9 = 0.3475$.

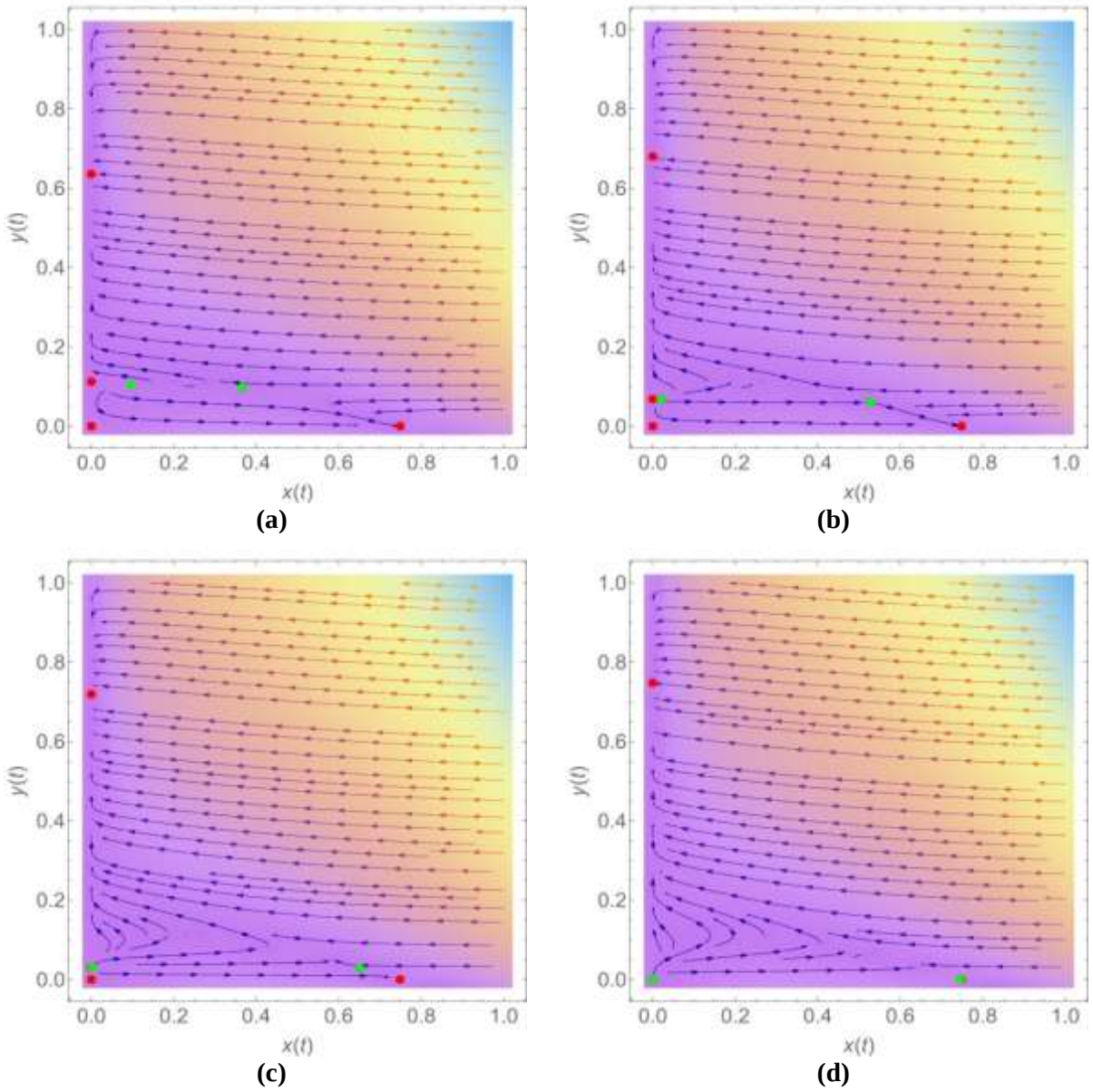

Figure 12- The right and left interior equilibrium points of set #2 (the points in green) go toward the predator-free and prey-free equilibria respectively, when the value of k_9 decreases toward zero, **(a)** $k_9 = 0.1$ **(b)** $k_9 = 0.07$ **(c)** $k_9 = 0.04$ **(d)** $k_9 = 0.0155$.

8. Discussion and Conclusions

In this study, a modified Leslie-Gower predator-prey model is proposed and discussed. Fear of predation and harvesting are both factored into the model's design and studied. According to Holling type-II functional response, which is also used to characterize the harvesting process, the predator consumes food. The solution's positivity and boundlessness have been demonstrated. All of the system's probable equilibrium positions are identified. These equilibrium points' local stability is explored, and their requirements are provided. The system shows it has several boundaries and interior equilibrium points, which complicates the study. The effect of changing the parameters on the model's dynamics is investigated by looking at the possibilities of local bifurcation types such as saddle-node, transcritical, and pitchfork bifurcation. Two sets of hypothetical data parameters are used to analyze the

system's global dynamics numerically. The existing equilibrium locations and the solution behavior surrounding them are depicted using phase portraits and direction fields. The system has a single globally asymptotically stable interior equilibrium point with two axial saddle-node equilibrium points and an unstable trivial equilibrium point for the data in set #1. The system has two unstable interior equilibrium points (one unstable spiral and the second is a saddle point) with three axial equilibrium points (two of which are locally asymptotically stable with their own basin of attraction for each of them and the third point is a saddle point) and a saddle-node trivial equilibrium point for data set #2. This ensures that the system's dynamics are rich, and the number of equilibrium points is determined by the data parameters. The impact of fear rate on the system's dynamics is also explored. For set # 1 data, increasing fear rate produces a gradual decrease in prey population until the system reaches prey extinction, and the interior equilibrium point coincides with the prey-free equilibrium point, which becomes globally asymptotically stable. In the set #2 data, however, raising the fear rate causes the two inner equilibrium points in the positive quadrant to be combined, resulting in a saddle-node point. According to the preceding discovery, fear rate acts as a bifurcation parameter, causing extinction in prey species when its value rises above a certain threshold. When the value of the catchability coefficient of the prey increases, similar observations are made as with the fear rate. Furthermore, when using set # 1 data, as the value of the predator's catchability coefficient increases, the system behaves similarly to that obtained when increasing the value of the prey's catchability coefficient, except that the interior equilibrium point combines with the predator-free equilibrium point, which then becomes globally asymptotically stable. The system behaves similarly when using set # 2 data. Finally, given set # 2 data, decreasing the predator species' catchability coefficient causes each of the interior equilibrium points to be combined with the nearest axial equilibrium point, and the system's solution approaches asymptotically to the prey-free equilibrium point.

Reference

[1] A. J. Lotka, *Elements of physical biology, Williams & Wilkins*, 1925.

[2] V. Volterra, *Variazioni e fluttuazioni del numero d'individui in specie animali conviventi, Mem Accad Linc* 2, 1926.

[3] Q. Yue, "Dynamics of a modified Leslie-Gower predator-prey model with Holling-type II schemes and a prey refuge," *SpringerPlus*, vol. 5, no. 1, pp. 1-12, 2016.

[4] H. Zhang, Y. Cai, S. Fu and W. Wang, "Impact of the fear effect in a prey-predator model incorporating a prey refuge," *Applied Mathematics and Computation*, vol. 356, pp. 328-337, 2019.

[5] É. Diz-Pita and M. V. Otero-Espinar, "Predator-Prey Models: A Review of Some Recent Advances," *Mathematics*, vol. 9, no. 15, p. 1783, 2021.

[6] R. K. Naji and R. A. Hamodi, "The Dynamics of an Ecological Model With Infectious Disease," *Global Journal Of Engineering Science And Researches*, vol. 3, no. 8, pp. 69-89, 2016.

[7] A. K. Pal, "Effect of fear on a modified Leslie-Gower predator-prey eco-epidemiological model with disease in predator," *J. Appl. Math. & Informatics*, vol. 38, no. 5-6, pp. 375-406, 2020.

[8] R. Sivasamy, K. Sathiyanathan and K. Balachand, "Dynamics of a Modified Leslie-Gower Model With Gestation Effect And Nonlinear Harvesting," *Journal of Applied Analysis and Computation*, vol. 9, no. 2, pp. 747-764, 2019.

[9] A. S. Abdulghafour and R. K. Naji, "A study of a diseased prey-predator model with refuge in prey and harvesting from predator," *Journal of Applied Mathematics*, vol. 2018, pp. 1-17, 2018.

[10] M. Kaur, R. Rani, R. Bhatia, G. N. Verma and S. Ahirwar, "Dynamical study of quadrating harvesting of a predator–prey model with Monod–Haldane functional response," *Journal of Applied Mathematics and Computing*, vol. 66, no. 1, pp. 397-422, 2021.

[11] E. Rahmi, I. Darti, A. Suryanto and Trisilowati, "A Modified Leslie--Gower Model Incorporating Beddington--DeAngelis Functional Response, Double Allee Effect and Memory Effect," *Fractal and Fractional*, vol. 5, no. 3, p. 84, 2021.

[12] S. Al-Momen and R. K. Naji, "The Dynamics of Sokol-Howell Prey-Predator Model Involving Strong Allee Effect," *Iraqi Journal of Science*, vol. 62, no. 9, pp. 3114-3127, 2021.

[13] F. J. Solis and R. A. Ku-Carrillo, "Birth Rate Effects on an Age-Structured Predator-Prey Model," Abstract and Applied Analysis, vol. 2015, pp. Article ID 241312, 7 pages, 2015.

[14] S. Li and Z. Xiong, "Bifurcation analysis of a predator-prey system with sex-structure and sexual favoritism," *Advances in Difference Equations*, no. 1, pp. 1-24, 2013.

[15] N. Bolohan, V. Leblanc and F. Lutscher, "Seasonal dynamics of a generalist and a specialist predator on a single prey," *Mathematics in Applied Sciences and Engineering*, vol. 2, no. 2, pp. 103-122, 2021.

[16] O. A. Nev and H. A. van den Berg, "Holling Type I versus Holling Type II functional responses in Gram-negative bacteria," *Transactions of Mathematics and its Applications*, vol. 2, no. 1, pp. 1-19, 2018.

[17] X. Liu and L. Chen, "Complex dynamics of Holling type II Lotka–Volterra predator–prey system with impulsive perturbations on the predator," *Chaos, Solitons and Fractals*, vol. 16, no. 2, pp. 311-320, 2003.

[18] L. Cheng and H. Cao, "Bifurcation analysis of a discrete-time ratio-dependent predator-prey model with Allee effect," *Communications in Nonlinear Science and Numerical Simulation*, vol. 38, pp. 288-302, 2016.

[19] X.-Y. Meng and J.-G. Wang, "Analysis of a delayed diffusive model with Beddington--DeAngelis functional response," *International Journal of Biomathematics*, vol. 12, no. 4, pp. 103-122, 2019.

[20] P. Leslie and J. Gower, "The properties of a stochastic model for the predator-prey type of interaction between two species," *Biometrika*, vol. 47, no. 3/4, pp. 219-234, 1960.

[21] M. Aziz-Alaoui and M. D. Okiye, "Boundedness and global stability for a predator-prey model with modified Leslie-Gower and Holling-type II schemes," *Applied Mathematics Letters*, vol. 16, no. 7, pp. 1069-1075, 2003.

[22] S. Yu, "Global stability of a modified Leslie-Gower model with Beddington-DeAngelis functional response," *Advances in Difference Equations*, no. 1, pp. 1-14, 2014.

[23] A. Singh and P. Malik, "Bifurcations in a modified Leslie-Gower predator-prey discrete model with Michaelis-Menten prey harvesting," *Journal of Applied Mathematics and Computing*, no. 67, pp. 1-32, 2021.

[24] R. Gupta and P. Chandra, "Bifurcation analysis of modified Leslie-Gower predator-prey model with Michaelis-Menten type prey harvesting," *Journal of Mathematical Analysis and Applications*, vol. 398, no. 1, pp. 278-295, 2013.

[25] C. Arancibia–Ibarra, J. Flores and P. v. Heijster, "Stability analysis of a modified Leslie-Gower predation model with weak Allee effect on the prey," *arXiv, p. arXiv preprint arXiv*:2009.02478, 2020.

[26] B. Leard, C. Lewis and J. Rebaza, "Dynamics of ratio-dependent predator–prey models with non-constant harvesting," *Discrete Contin. Dyn. Syst. Ser*., no. 2, pp. 303-315, 2008.

[27] J. Mena Lorca, E. Gonzalez Olivares and B. Gonzalez Yanez, "The Leslie Gower predator prey model with Allee effect on prey: a simple model with a rich and interesting dynamics," in *International Symposium on Mathematical and Computational Biology*, 2006.

[28] D. Jana, R. Pathak and M. Agarwal, "On the stability and Hopf bifurcation of a prey-generalist predator system with independent age-selective harvesting," *Chaos, Solitons & Fractals*, no. 83, pp. 252-273, 2016.

[29] R. Gupta, P. Chandra and M. Banerjee, "Dynamical complexity of a prey-predator model with nonlinear predator harvesting," *Discrete & Continuous Dynamical Systems-B*, vol. 20, no. 2, pp. 423-443, 2015.